Heat transfer effect on the non-wetting liquid drop by using the Shan-Chen LBM model

S. CHANNOUF[a], M. JAMI[a], A. MEZRHAB[a], J.BENHAMOU[a]

a. Laboratoire de Mécanique et Energétique, Université Mohammed Premier, Faculté des Sciences, 60000 Oujda, Maroc

Abstract :

In the last years, the lattice Boltzmann method (LBM) have been widely used as a solver for simulating hydrodynamics problems. Thus, this method is used to simulate two-phase flows in a 2D computational domain by using the pseudo-potential model proposed by Shan-Chen [1] in (1993) which is called Shan-Chen LBM model. Firstly, we validated our code with the work of Huang et al.[2] who have modeled the wettability phenomena of a liquid drop. Secondly, we have studied the effect of natural thermal convection on a liquid drop inside a differentially heated square cavity by fixing the density of the surface wetting on 2 and by varying the Rayleigh number from 10^3 *to* 10^6*. Results show that the liquid drop moves under the effect of gas flow caused by the convection and it evaporates by exchanging heat with gas.*

Key words: lattice Boltzmann method, Shan-Chen LBM model, two-phase flows, wettability phenomena, natural thermal convection.

1 Introduction

The Lattice Boltzmann Method is one of the most powerful explicit computational technique for modeling the two-phase flows and also a numerical approach of the computational fluid dynamics (CFD) in fluid engineering which is based on the mesoscopic kinetic equations(The kinetic Theory of gases). The Lattice Boltzmann method (LBM) has emerged as a promising tool for are solving the hydrodynamic Navier–Stokes equations and simulating complex fluid flow.

Several studies have been conducted to simulate the two-phase LBM flows, the earliest one is the color-gradient model proposed by Gunstensen et al. [3] (1991), which is based on the Rothman–Keller (1988) (RK) multiphase lattice gas model [4]. The Shan–Chen (SC) model (1993) appeared soon after and is based on incorporation of an attractive or repulsive force, which leads to phase separation. The free-energy (FE) model was proposed by Swift et al. [5] (1995), in this model the thermodynamic issue of the non-monotonic equation of state is incorporated into the pressure tensor in the N–S equations. Also, another model is based on the interface tracking method and is proposed by He-Chen-Zhang (HCZ) [6] (1999).

In our study, The Shan-Chen (1993) LBM model has been used to simulate two-phase flows, even though the simulation of more phases is possible. The basic idea behind the Shan-Chen

model lies in the introduction of an interaction force between a node of the lattice and its "nearest neighbours", which is able to trigger phase separation in certain conditions. Two forces are involved, the adhesive force will appear to describe the interaction between the fluid and the solid surface and the cohesive force for the fluid-fluid interface, which are commonly used to determine the wettability (the degree of wetting) in terms of the solid-fluid contact angle.
This paper is organized as follows. In Section 2, we will illustrate the physical problem, the method for measurement of the contact angle. In section 3, we will present the validation and discuss our results.

2 Methodology

2.1 The Shan-Chen LBM Model

In the current study, the same configuration is performed for both distribution functions representing the fluid flow $f_i(\boldsymbol{x}, t)$ and the temperature field $g_i(\boldsymbol{x}, t)$, respectively. The two-dimensional nine velocity D_2Q_9 model is adopted for the evolution process of both distribution functions which is represented as :

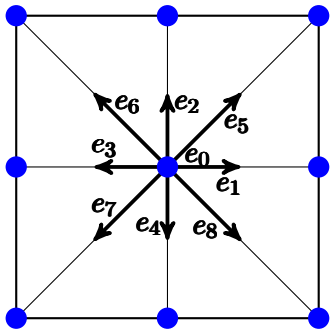

Figure 1: ***Illustration of a lattice node of the*** D_2Q_9 ***Model.***

The Bhatnagar, Gross and Krook (BGK) approximation scheme for collision operator is adopted for both collision and streaming steps which is given by the following equation :

$$f_i(\boldsymbol{x} + \boldsymbol{e}_i\delta t, t + \delta t) = f_i(\boldsymbol{x}, t) - \frac{\delta t}{\tau}(f_i(\boldsymbol{x}, t) - f_i^{eq}(\boldsymbol{x}, t)) \tag{1}$$

$f_i(\boldsymbol{x}, t)$ represents the distribution function, τ is the relaxation time that it related to the kinematic viscosity as $\nu = c_s^2(\tau - 0.5\delta t)$, $c_s = 1/\sqrt{3}$ represents the speed of sound and $f_i^{eq}(\boldsymbol{x}, t)$ is the equilibrium distribution function defined by :

$$f_i^{eq}(\boldsymbol{x}, t) = \rho(\boldsymbol{x}, t)w_i[1 + \frac{\boldsymbol{e}_i.\boldsymbol{u}^{eq}}{c_s^2} + \frac{(\boldsymbol{e}_i.\boldsymbol{u}^{eq})^2}{2c_s^4} - \frac{(\boldsymbol{u}^{eq})^2}{2c_s^2}] \tag{2}$$

w_i represents the weight factors :

$$w_i = \begin{cases} 4/9 & i = 0 \\ 1/9 & i = 1, 2, 3, 4 \\ 1/36 & i = 5, 6, 7, 8 \end{cases}$$

The equilibrium velocity $\boldsymbol{u}^{eq}$ is given by :

$$\boldsymbol{u}^{eq} = \boldsymbol{u}^{'} + \frac{\tau \boldsymbol{F}}{\rho} \tag{3}$$

$\boldsymbol{F} = (F_x, F_y)$ is the total force acting on the fluid including fluid-fluid interaction $\boldsymbol{F}_{sc}$ (cohesive force) and fluid-solid interface $\boldsymbol{F}_{ads}$ (adhesive force). The velocity $\boldsymbol{u}^{'}$ is given by :

$$\boldsymbol{u}^{'} = \sum_i \frac{f_i \boldsymbol{e}_i}{\rho} \tag{4}$$

The interaction force $\boldsymbol{F}_{sc}$ is calculated over nearest neighbours of the pseudopotential function ψ by :

$$\boldsymbol{F}_{sc}(\boldsymbol{x}, t) = -G\psi(\boldsymbol{x}, t) \sum_i w_i \psi(\boldsymbol{x} + \boldsymbol{e}_i \delta t, t) \boldsymbol{e}_i \tag{5}$$

G is the coefficient that controls the strength of the inter-particle force. It is attractive for $(G < 0)$ and repulsive for $(G > 0)$. The function $\psi = \psi(\rho)$ depends on the local density as follows :

$$\psi(\rho) = \rho_0(1 - \exp(-\rho/\rho_0)) \tag{6}$$

ρ_0 is the reference density. An explicit formula for the pseudopotential function ψ can be defined related to the equation of state (EOS) according to Yuan and Schaefer (2006) [7] by :

$$\psi = \sqrt{\frac{2(P - \rho c_s^2)}{G c^2}} \tag{7}$$

The choice of EOS can reflect the relationship between the pressure, temperature and density. According to Ginzburg and Adler [8], the flow velocity of fluid and the density can be obtained by the following equations :

$$\boldsymbol{u}(\boldsymbol{x}, t) = \boldsymbol{u}^{'} + \frac{\delta t \boldsymbol{F}}{2\rho} \quad ; \quad \rho(\boldsymbol{x}, t) = \sum_i f_i \tag{8}$$

The fluid-solid adhesive force is calculated by :

$$\boldsymbol{F}_{ads}(\boldsymbol{x}, t) = -G\psi(\rho) \sum_i w_i \psi(\rho_w) s(\boldsymbol{x} + \boldsymbol{e}_i \delta t, t) \boldsymbol{e}_i \tag{9}$$

The pseudopotential parameter at the wall $\psi(\rho_w)$ is used to adjust the different properties of the wetting surface. ρ_w is not used as real value of density of the wetting surface and $s(\boldsymbol{x} + \boldsymbol{e}_i \delta t, t)$ is a switch function, which is equal to 1 for a solid phase or 0 for fluid phase. The body force responsible to the generation of the temperature field (natural convection) is added to the collision process as :

$$f_i(\boldsymbol{x} + \boldsymbol{e}_i \delta t, t + \delta t) = f_i(\boldsymbol{x}, t) - \frac{\delta t}{\tau}(f_i(\boldsymbol{x}, t) - f_i^{eq}(\boldsymbol{x}, t)) + \Delta t F_i(\boldsymbol{x}, t) \tag{10}$$

Where, $F_i(\boldsymbol{x}, t)$ represents the gravity force and it can be defined as : $F_i(\boldsymbol{x}, t) = 3\rho\beta w_i g \Delta T \boldsymbol{e}_y$. Where, g is the acceleration due to gravity, β is the thermal expansion coefficient and ΔT is the temperature difference between the high and low temperature walls.

Essential Parameters :

In this study, the Redlich-Kwong (R–K) EOS model is considered to describe the relationship between the pressure, temperature and density. It is expressed by :

$$p = \frac{\rho RT}{1 - b\rho} - \frac{a\rho^2}{\sqrt{T}(1 + b\rho)} \tag{11}$$

In our simulations, the parameters are set to be $a = 2/49$, $b = 2/21$, $R = 1$ and $T = 0.85T_c$. Where, T_c is the critical temperature. The coexisting densities are the liquid density $\rho_l = 6.06$ and the gas density $\rho_g = 0.5$, the contact angle is the most important parameter used to quantify the wettability of a liquid drop [9, 10]. It can be evaluated geometrically as :

$$\theta = \arctan\left(\frac{b}{2(r - h)}\right) \tag{12}$$

Where, b and h represent the base and the height of the liquid drop of radius r respectively

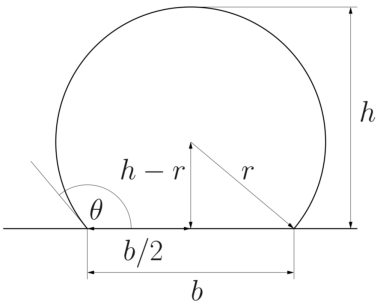

Figure 2: ***Geometrical measurement of the contact angle.***

as shown in Figure 2. In turn, the radius r is expressed by $r = b^2/8h + h/2$.
The basic dimensionless parameters of fluid flows are Rayleigh R_a and Prandtl P_r numbers which are defined as [11]:

$$R_a = \frac{g\beta\Delta T}{\nu\alpha}L_x^3 \;\; ; \;\; P_r = \frac{\nu}{\alpha} \tag{13}$$

Where g is the acceleration due to gravity, β is the thermal expansion coefficient, ΔT is the temperature difference between the high and low temperature walls which is equal to unity and L_x is the distance between them. α and ν are the thermal diffusivity and the kinematic viscosity, respectively.

2.2 Configuration of the numerical problem

Figure 3 presents the geometry and the boundary conditions of a two-dimensional differentially heated square cavity placed in a gravity field simulated bv the SC LBM model. The computational numerical domain used in this study is (600×600). The temperatures of the left and the right vertical walls of the domain are maintained at $T_{hot} = 0.5$ and $T_{cold} = -0.5$, respectively. The upper and lower horizontal walls have been considered as adiabatic. For the fluid flow, the no-slip boundary (reflection of all distribution functions at the wall in the opposite direction) is considered for the upper and lower boundaries, the bounce-back condition is

selected for side walls (bounce-back for the right wall i.e. $f_1(\boldsymbol{x},t) = f_3(\boldsymbol{x},t)$, $f_5(\boldsymbol{x},t) = f_7(\boldsymbol{x},t)$, $f_8(\boldsymbol{x},t) = f_6(\boldsymbol{x},t)$). The laminar gas flow can be described by assuming that the gas is newtonian, incompressible and satisfies the Boussinesq approximation. Midway between the vertical walls a liquid drop of radius $r = 30lu$ (lattice unit) is positioned.

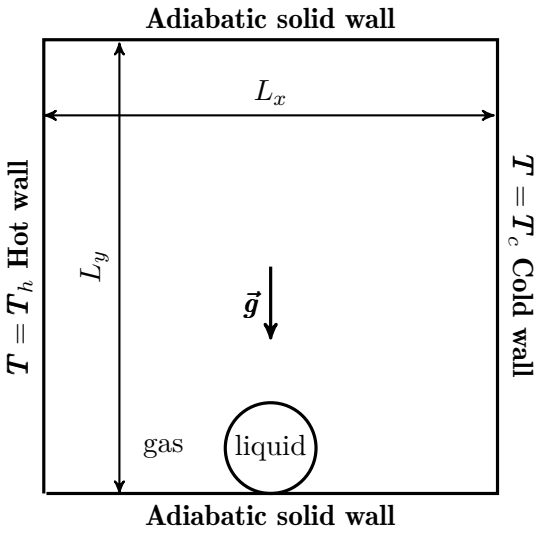

Figure 3: ***Illustration of the physical problem used in the simulation.***

3 Results and discussions

3.1 Validation

Our results agree well with those obtained by Huang et al.(2009), which are presented that when the density of the wetting surface ρ_w takes values between the density of the gas (ρ_g) and the density of the liquid (ρ_l), $\rho_g \leq \rho_w \leq \rho_l$. The contact angle θ takes values between $0 \leq \theta \leq 180°$. The measure of the contact angle usually indicates that wetting of the surface is unfavorable for $90 < \theta \leq 180°$ or it is favorable for $\theta \leq 90°$. Figure (3-a) shows that the wetting of the surface is unfavorable (non-wetting phase) for $\theta = 148.8°$ and $\rho_w = 2$, so the liquid drop will minimize its contact with the surface and form a compact liquid droplet. However, in Figure (3-b) the wetting of the surface is favorable (wetting phase) for $\theta = 11.6°$ and $\rho_w = 5.5$, so the liquid drop will spread over a large area on the surface.

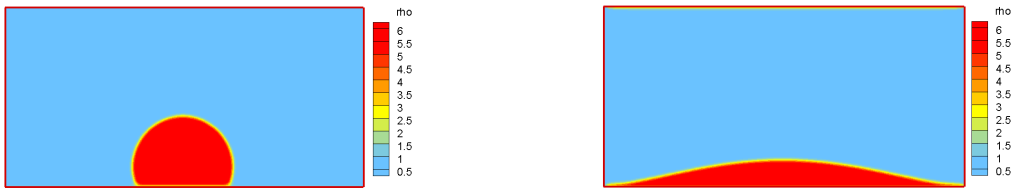

(a) *(b)*

Figure 4: ***Different wetting situations : (a) non-wetting case with a contact angle of greater than*** $90°$***, (b) wetting case where the droplet spreads out over a solid surface.***

3.2 Results

In our simulation, we present the influence of the gas's motion created by natural convection on the liquid drop for different Rayleigh numbers ($10^3 \leq R_a \leq 10^6$) as shown in figure 4. From this Figure, it seen that for all values of R_a, the heated gas rises along the left wall, encounters the top adiabatic wall, travels towards the cold wall, comes down and recirculates inducing a steady clockwise rotational flow. This recirculation pushes the liquid drop towards the left wall and this behavior is more clearer for high Rayleigh number. The liquid drop keeps the same shape while moving. However its radius decreases owing to the heat exchange between the gas trapped in the cavity and the liquid droplet. Indeed, the drop is evaporated and it becomes smaller than its initial shape. As R_a reaches 10^6, the flow moves faster as natural convection is intensified. The liquid drop moves to take place next to the hot wall and it deforms under the effect of gas pressure.

In an evaporation process, a mass transfer occurs, which means liquid meniscus including a triple contact line has a motion. Therefore, we need to consider a dynamic contact angle (advancing and receding contact angles) as shown in figure 2. Generally, the advancing contact angle will tend toward a lower value during evaporation. The evaporation time of the drop of liquid increases with increasing the Rayleigh number, this leads to an increase in the rate of transfer of heat by convection of the cooled gas coming from the cold wall.

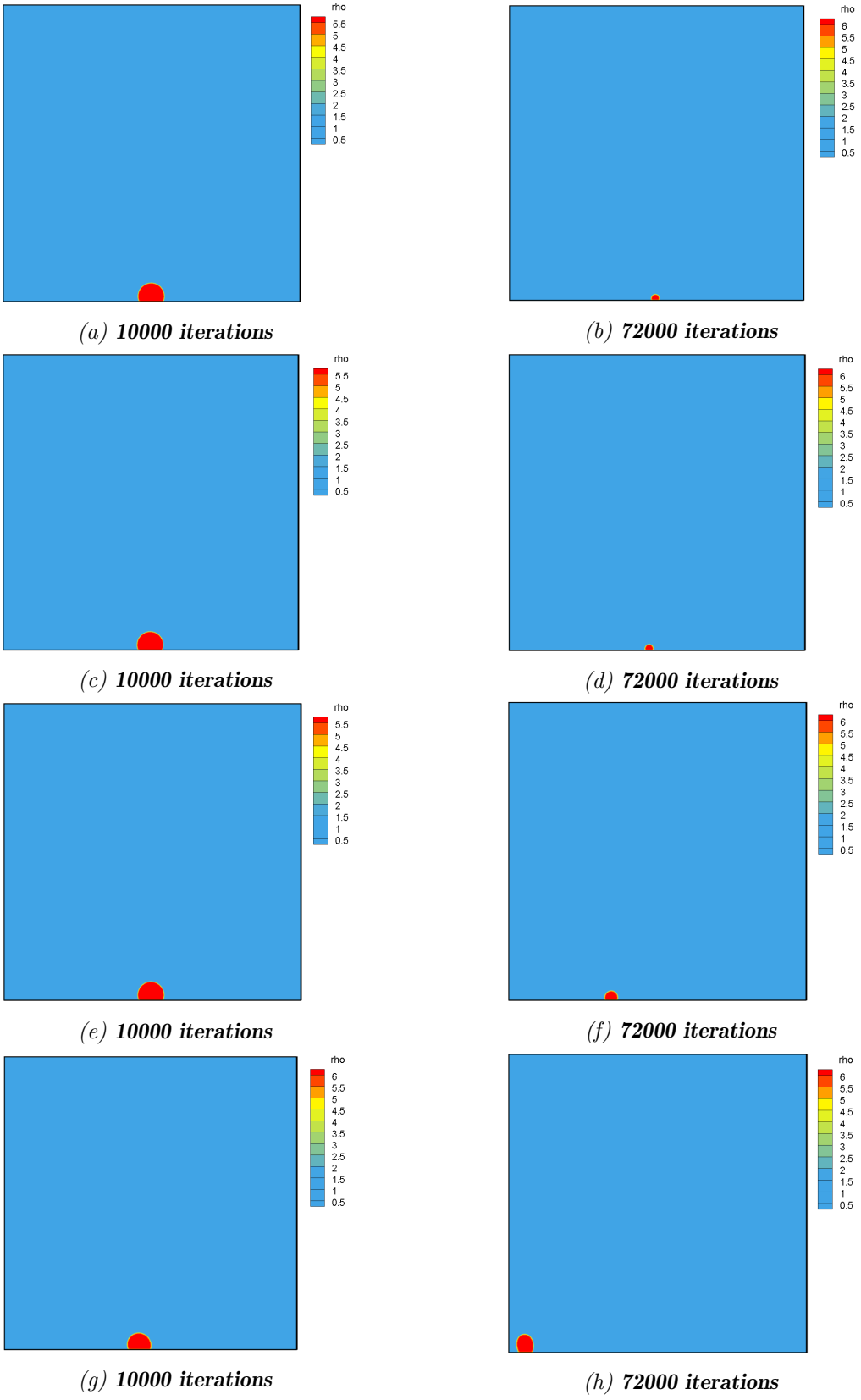

(a) **10000 iterations** (b) **72000 iterations**

(c) **10000 iterations** (d) **72000 iterations**

(e) **10000 iterations** (f) **72000 iterations**

(g) **10000 iterations** (h) **72000 iterations**

Figure 5: **Evaporation process of the liquid drop for** $P_r = 0.71$ **and for different Rayleigh numbers (a-b) :** $R_a = 10^3$**, (c-d) :** $R_a = 10^4$**, (e-f) :** $R_a = 10^5$**, (g-h) :** $R_a = 10^6$**.**

4 Conclusion

Numerical computations were performed to study the wettability-natural convection interactions of a liquid drop inside a square cavity differentially heated. The Shan-Chen LBM and Thermal LBM models are used. The main purpose of this study was to follow the evaporation process of a liquid drop by varying the Rayleigh number, R_a, and to verify the influence of laminar natural convection on the wettability phenomenon. The results were presented in the form of figures showing the evolution of the liquid drop over time. The results show that :

- The liquid drop size decreases with time steps for all Rayleigh numbers R_a.
- For $R_a \leq 10^5$, the liquid drop moves to take place next to the hot wall and it keeps its initial shape during process.
- For $R_a = 10^6$, the liquid drop moves to take place next to the hot wall and it deforms under the effect of gas pressure.
- The liquid drop radius decreases rapidly for low $R_a = 10^3$.

References

[1] X. Shan and H. Chen, Lattice boltzmann model for simulating flows with multiple phases and components, Physical Review E vol. 47 no. 3 (1993) 1815.

[2] H. Huang, Z. Li, S. Liu and X.-y. Lu, Shan-and-chen-type multiphase lattice boltzmann study of viscous coupling effects for two-phase flow in porous media, International journal for numerical methods in fluids vol. 61 no. 3 (2009) 341–354.

[3] Gunstensen, K. Andrew K, H. Daniel Rothman, Stéphane Zaleski, and Gianluigi Zanetti, Lattice Boltzmann model of immiscible fluids, Physical Review A 43 no. 8 (1991) 4320.

[4] Rothman, H. Daniel and Jeffrey M. Keller, Immiscible cellular-automaton fluids, Journal of Statistical Physics 52 no. 3-4 (1988) 1119-1127.

[5] Swift, R. Michael, W. R. Osborn and J. M. Yeomans, Lattice Boltzmann simulation of non-ideal fluids, Physical review letters 75 no. 5 (1995) 830.

[6] He, Xiaoyi, Shiyi Chen and Raoyang Zhang, A lattice Boltzmann scheme for incompressible multiphase flow and its application in simulation of Rayleigh–Taylor instability, Journal of Computational Physics 152 no. 2 (1999) 642-663.

[7] P. Yuan and L. Schaefer, Equations of state in a lattice boltzmann model, Physics of Fluids, vol. 18, no. 4, p. 042101, 2006.

[8] I. Ginzbourg and P. Adler, Boundary flow condition analysis for the three-dimensional lattice boltzmann model, Journal de Physique II, vol. 4, no. 2, pp. 191–214, 1994.

[9] Yuan, Yuehua and T. Randall Lee, Contact angle and wetting properties, Surface science techniques(Springer) vol. 51 (2013) 3-34.

[10] Schmieschek, Sebastian and Jens Harting, Contact angle determination in multicomponent lattice Boltzmann simulations, Communications in computational physics 9, United Kingdom, 2011, 1165-1178.

[11] A.A. Mohamad, Lattice Boltzmann method: fundamentals and engineering applications with computer codes, Springer Science Business Media, 2011.